ChemSearch Journal 15(2): 111 – 119, December, 2024
Publication of Chemical Society of Nigeria, Kano Chapter

Received: 07/09/2024 Accepted: 24/11/2024
http://www.ajol.info/index.php/csj

Solid State Synthesis, Characterization, Anti-Oxidant and Anti-Microbial Studies of some Guanine Complexes

Jafar, J., Na'aliya, J. and Sadiq, I. A.
Department of Pure and Industrial Chemistry, Bayero University, P.M.B. 3011 BUK, Kano-Nigeria
***Correspondence Email:** bignamejjjj@gmail.com

ABSTRACT

Metal(II) carbonates (Mn, Ni, Zn) were ground mechanochemically to produce guanine complexes.. Elemental analysis, infrared spectroscopy, melting/decomposition temperature determination and conductivity tests were used to characterize the synthesized complexes. The infrared spectroscopic analysis of the ligand shows a peak at 1674cm^{-1} which can be assign to the presence of azomethane in guanine while the shift to1566-1640 cm^{-1} confirmed bond formation from azo-group to metal, while the appearance of new peak at 559-592cm^{-1} and 440-452cm^{-1} was due to deprotonated amine(-NH) and ring nitrogen respectively confirm complexation. The guanine ligand's melting point temperature of 360^{0}C indicates its stability at high temperatures, whereas the complex's decomposition temperature of over 360^{0}C indicates its extreme stability. Comparing the complexes to the theoretical values, conductivity measurement reveals that they are non-electrolytic (29.0-60.6 × 10^{-6} Ω^{-1}cm^{2} mol^{-1}). At high concentrations (4000 µg/disc and 500 µg/disc), the ligand and its corresponding complexes demonstrated antimicrobial properties against a variety of bacteria and fungi, and their anti-oxidant activity was assessed using the IC50 range (0.00–98.4µg/ml).

Keywords: Anti-Microbial, Anti-oxidant, Guanine, Mechanochemical

INTRODUCTION

Using a mortar and pestle, mechanochemical solvent-free organic reactions have become a potent substitute for synthetic processes in solution. The possible use of extremely sensitive reagents or intermediates for mechanochemical transformations under ambient circumstances is still elusive, and the advantages of mechanochemistry in the context of chemistry have not yet been well investigated (Rina, 2022).

Iron (Fe)-tin (Sn) intermetallic compound ($FeSn_2$) was reported to be synthesized by using a two-step process of mechanical alloying and liquid phase sintering. In the first, mixtures of as-received Fe and Sn powders were mechanically alloyed. In the second, the as-received Fe powder was pre-milled first and the as-received Sn powder was then added and mechanically alloyed. The two-step process using the second mechanical alloying procedure performed better; it synthesized more of the $FeSn_2$ intermetallic compound(Nattaya *et al*., 2017).

A Schiff base ligand, 2-((E)-((4-(((E)-benzylidene) amino) phenyl) imino) methyl)-nap hthalene-1-ol, was prepared by the reflux condensation of p-phenylenediamine with 2-hydroxy-1- naphthaldehyde and benzaldehyde. Metal complexes were prepared by reacting the ligand with metal salts: V, Cr, Mn, Fe, Co, Ni, and Zn. The ligand and its metallic complexes were characterized by various techniques such as elemental analysis, AAS, NMR, IR value range from 405-688cm^{-1}, UV–Vis, TGA, DTA, XRD and TEM (Thamer *et al*., 2022).

Chiral N-(2-hydroxy-1-naphthylidene) amino acid Cu (II) complexes were synthesized and characterized by various spectroscopic techniques FT-IR, UV−vis, electron paramagnetic resonance, electrospray ionization-mass spectrometry, and circular dichroism) and single X-ray crystal diffraction analyses. To understand the selectivity and enantiomeric behaviour of the complexes, binding interaction with ct-DNA and tRNA biomolecules was investigated by widely employed optical and hydrodynamic techniques. The binding experiments demonstrated that the complexes interact strongly via the intercalative mode with preferential binding toward the tRNA biomolecule compared to ct-DNA. In vitro cytotoxic activities of complexes show that the complex with highest cytotoxicity, and is selectively targeted toward the human breast cancer cell line (MCF-7) with a GI50 value of <1 µM. The results suggest that the L-enantiomeric complexes are more avid binders toward the tRNA molecule and showed better cytotoxicity. The IR bands corresponding to ν(−C=N) vibrations for complexes were recorded in the range of 1637−1642cm^{-1}. The Far-IR spectra of the complexes showed bands in the regions 574−550cm^{-1} and 486−479cm^{-1}, which were assigned to ν(M−N) and ν(M−O) stretching vibrations respectively (Siffeen *et al*., 2019).

The green synthesis for the fabrication of polyhedral oligomeric silsesquioxane-supported N-heterocyclic carbenes/imidazolium salts on palladium(II) complexes; Pd(II)-MPIm-POSS composite by solid-state annealing between $Pd(OAc)_2$ and octakis(3-(1-methylimidazolium) propyl) octasilsesquioxane without added base. Subsequently, arylboronic acid based in situ or ex situ reduction of the complex in aqueous ethanol produces polyhedral oligomeric silsesquioxane supported N-heterocyclic carbenes/imidazolium salts on palladium nanoparticles; Pd(0)-nano-POSS (2) composite, consisting of monodispersed and N-heterocyclic carbene (NHC) stabilized Pd nanoparticles of very small size (3.0 1.5 nm). Nanocatalyst is a highly efficient and easily recyclable homogeneous catalyst (Sudip *et al*., 2016).

Solid-state anaerobic digestion (SS-AD) was commonly used to treat feedstocks with high solid content such as municipal solid waste and lignocellulosic biomass. Compared to liquid state anaerobic digestion (LS-AD), SS-AD has multiple advantages including high organic loading, minimal digestate generated, and low energy requirement for heating. However, the main disadvantages limiting the efficiency of SS-AD are long solid retention time, incomplete mixing, but the performance can be enhanced by feedstock pretreatment, co-digestion, and supplement of additives such as biochar (Haoqin and Zhiyou , 2019).

Parkia speciosa (petai) pods are rarely used and considered as waste despite their phenolic and flavonoid content. Phenolic and flavonoid content in plants is known to exhibit antioxidant activity. The antioxidant potential of petai pods using DPPH method. Analysis showed the IC50 of petai pods ethanolic extract was 75.72 ppm, which indicate strong acting antioxidant (Najma *et al*., 2019).

Oxidative stress is a condition where reactive oxygen/nitrogen species (ROS/RNS) overpower an organism's antioxidant defenses, leading to oxidative damage, tissue injury, and cellular death. Measuring antioxidant activity is crucial for diagnosing and treating diseases, comparing foods, and controlling variations. However, standardized methods for measuring antioxidant capacity are lacking in medical diagnosis and treatment. The complexities of antioxidant applications require careful analysis of chemistry, reaction mechanisms, and specificity. There is currently no widely adopted "total antioxidant parameter" for labeling food and biological fluids, highlighting the need for standardized methods to measure TAC levels directly from plant-based food extracts and biological fluids (Resat *et al*., 2016).

Fermented wheat, extracted using acidified water, 70% acetone, and 70% ethanol, showed enhanced antioxidant properties compared to unfermented wheat. The acetone extract had the highest antioxidant content and lowest IC50 values. Fermentation with Cordyceps militaris can be used to develop wheat as a health food or ingredient with multi-functional properties, potentially used in the food industry as a natural antioxidant (Zuofa *et al*., 2012).

A new series of metal complexes with 1-(2-methylphenyl)-4,4,6-trimethyl pyrimidine-2-thione (**2-HL1**) and 1-(4-methylphenyl)-4,4,6-trimethyl pyrimidine-2-thione (**4-HL2**) ligands, [M(mppt)2(H_2O) n] (M(II) = Cu, Mn, Co; n = 2 and M(II) = Ni, Zn; n = 0) have been synthesized using mechanochemical protocol. The complexes have been framed as [$M(mppt)_2(H_2O)$ n] due to 1:2 (metal: ligand) nature of these metal complexes. The structures of the complexes were further confirmed on the basis of elemental analysis, Magnetic susceptibility measurements, electronic, infrared, far infrared, proton NMR, Mass spectral moment and thermogravimetric analyses (Pooja *et al*., 2020).

One-pot solvent free preparation of some new transition metal complexes of omeprazole (OMP), followed by their characterization and in vitro applications as anti-*Helicobacter pylori* agents and urease inhibitors. The complexes were characterized by elemental analyzer, IR, Powder X-Ray diffraction, ^{1}H-NMR,^{13}C-NMR and mass spectrometric and thermal methods, which elucidated that the complexes have the general formula [ML] X where M ═ Zn, Ni, Cu and X═ CH_3COO^- and [ML] X. H_2O, where M ═ Co, X═ CH_3COO^-. The complexes exhibited antibacterial activity against selected strains of Gram +ve and Gram –ve bacteria including *Staphylococcus aureus* (ATCC 29213), *S. epidermidis* (ATCC 12228), *Escherichia coli* (ATCC 12435), *Proteus vulgaris* (NCTC 4175), *Pseudomonas aeruginosa* (ATCC 49189) and fifteen local isolates and two reference strains of *H. pylori*. Zinc omeprazole (Zn-OMP), cobalt omeprazole (Co-OMP) and copper omeprazole (Cu-OMP), all exhibited potent and selective anti-H. pylori activity in the range of 1.0-128 μgmL^{-1} (Muhammad *et al*., 2018).

Propolis, a honeybee-produced mixture, has been studied for its biological properties and chemical composition. Mexican brown propolis has been studied for its antioxidant activity and cytotoxic activity. Twelve compounds were identified, including nonanal, pinene, neryl alcohol, and pinene. EEP showed better anti-proliferative effects on glioma cells and decreased proliferation and viability in cervical cancer cells, but its effectiveness was lower compared to cisplatin (Fausto, *et.al*., 2020).

A series of new metal complexes of the general formula [M $(NCCH_2CH_3)_6$] [B $(C_6F_5)_4]_2$, where M: Cu, Fe, Co, Ni, Zn, Mn, have been synthesized. The complexes are characterized via IR, TGA, NMR and Elemental Analysis. GC–MS have been used to determine the purity of the

reactions and the yield of the final products. These complexes have been applied as catalysis on different olefins for cyclopropanation reaction in homogenous phase. Complex of $[Cu(CH_3CH_2CN)_6][B(C_6F_5)_4]_2$ has shown the highest activity on different olefins. Their biological activities against a number of pathogenic bacteria have been screened and most of the complexes have shown moderate activities against Gram positive and low activities against Gram negative(Abdulaziz *et al*., 2019).

The syntheses and characterization of novel octacationic and hexadecatrienoic phthalocyanines(Pcs) was reported, with the aim of enhancing singlet oxygen generation efficiencies and hence antimicrobial activities, these phthalocyanines (Pcs) (including their neutral counterpart) are conjugated to Ag nanoparticles (Ag NPs). The obtained results show that the conjugate composed of the neutral phthalocyanines has a higher loading of phthalocyanines as well as a greater singlet oxygen quantum yield enhancement (in the presence of Ag NPs) in DMSO. The antimicrobial efficiencies of the phthalocyanines and their conjugates were evaluated and compared on *S. aureus, E. coli* and *C. albicans*. The cationic phthalocyanines possess better activity than the neutral phthalocyanines against all the microorganisms with the hexadecacationic phthalocyanines being the best. Therefore increase in the number of cationic charges on the reported phthalocyanines results in enhanced antimicrobial activities, which is maintained even when conjugated to Ag nanoparticles. The high activity and lack of selectivity of the cationic phthalocyanines when conjugated to Ag NPs against different microorganisms make them good candidates for real life antimicrobial treatments(Panel *et al.,* 2021) The study of antioxidants and their implications in various fields, from food engineering to medicine and pharmacy, is of major interest to the scientific community. The antioxidant activity, detection mechanism, applicability, advantages and disadvantages of these methods, which include the transfer of a hydrogen atom, Oxygen Radical Absorption Capacity (ORAC) test, the Hydroxyl Radical Antioxidant Capacity (HORAC) test, the Total Peroxyl Radical Trapping Antioxidant Parameter (TRAP) test, and the Total Oxyradical Scavenging Capacity (TOSC) test. The tests based on the transfer of one electron include the Cupric Reducing Antioxidant Power (CUPRAC) test, the Ferric Reducing Antioxidant Power (FRAP) test, the Folin–Ciocalteu test. Mixed tests, including the transfer of both a hydrogen atom and an electron, include the 2,20 -Azinobis-(3-ethylbenzothiazoline-6-sulfonic acid (ABTS) test, and the [2,2-di(4-tert-octylphenyl)-1-picrylhydrazyl] (DPPH) test (Irina and Constantin 2021).

A series of Ni (II), Co (II) and Cu (II) complexes were synthesized with excellent yields via a one-pot ball milling chelation reaction of those metals and β-diketone. The synthesized compounds were interpreted by using various spectroscopic techniques [infrared (IR), ^{1}H-NMR, ^{13}C-NMR, UV–visible, electron spin resonance (ESR) and mass spectrometry] together with some physical studies (molar conductance and magnetic susceptibility). The outcomes data displayed that the ligands acted as neutral and/or mono-negative bidentate ligands. Also, the *in vitro* antimicrobial assay was done by using the well diffusion method for ligands and their corresponding complexes. The physical and analytical outcomes data of *β*-diketone and their metal complexes are in good agreement with theoretical values. In addition, the molar conductance of the prepared compounds suggested the behaviour of the non-electrolytes (Zaky and Fekri, 2019).

Novel complexes of Co(II) and V(IV) where synthesized from (E)2-(((2-((2-hydroxyethyl) amino) quinolin-3-yl) methylene) amino) ethan-1-ol ligand (L), cobalt (II) chloride hexahydrate, and vanadyl (IV) sulfate in methanolic solutions. The ligand and the complexes were characterized by ^{1}HNMR spectroscopy,^{13}C NMR spectroscopy, UV−visible spectroscopy, fluorescence spectroscopy, FT-IR spectroscopy, powder X-ray diffraction (PXRD), scanning electron microscopy−energy dispersive X-ray spectroscopy (SEM−EDX), mass spectroscopy (MS), thermal analysis, and molar conductance. The antibacterial activities of the free ligand and its complexes were evaluated using a paper disk diffusion method. The complexes have better percent activity index than the free ligand. Furthermore, the antioxidant activities of the free ligand and its metal complexes were also determined in vitro using 2,2-diphenyl-1-picrylhydrazyl. The ligand exhibited less in vitro antioxidant activity than its transition metal complexes, in which the cobalt complex has a better antioxidant activity with half-inhibitory concentrations (IC_{50} of 16.01 μg/ mL) than the ligand and the vanadium complex. Quantum molecular descriptors from the DFT calculations further support the experimental results. Molecular docking analysis also shed more light on the biological activities of the novel cobalt and vanadium complexes. The conductivity tests revealed their non-electrolytic nature with molar conductance values of 8.47 ± 0.25 $\Omega^{-1}mol^{-1}cm^2$ and 13.20 ± 0.59 $\Omega^{-1}mol^{-1}cm^2$ for the complexes (Tadewos *et al*., 2022).

Cancer continues to be responsible for the deaths of millions of people worldwide each year. Current treatment options are diverse, but low success rates, particularly for those with late-stage cancers, continue to be a problem for clinicians and their patients. The effort by researchers globally to find alternative treatment options is ongoing. The

synthesis of transition metals inorganic complexes with anticancer therapies, specifically those with photoactive and luminescent properties offer distinct advantages compared to wholly organic compounds in both chemotherapeutics and luminescence properties. The result shows that the complexes have IC50 value range(0-100µg/ml) indicating good activity to monitor cellular localization to photodynamic therapy (Brondwyn and Janice, 2022).

MATERIALS AND METHODS

Materials

All chemicals and reagents obtained from Sigma Aldrich were used without further purification. After soaking in concentrated HNO_3, all glassware cleaned with soap, rinsed with purified water, and dried in an oven. A Melter balance type AB54 electrical device was used for the weighing process. Using a Fourier transform infrared spectrophotometer (FTIR-8400S) with a range of 4000-400cm^{-1}, infrared spectral analysis was determined. Electrical conductances were measured using a Jenway conductivity meter model 4010 with a range of 20–200µs. Microprocessor melting point equipment (WRS-IB) was used to determine melting points and decomposition temperature. Using the magnetic susceptibility balance MKI Sherwood Scientific Ltd., magnetic susceptibility was ascertained. Elemental analyses were calculated with Perkin Elmer's Series II CHNS/O 2400. A motor and pestle were used for the synthesis.

Methods

Synthesis of Guanine Complexes

Metal(II) carbonates (0.01mol) was ground with guanine (0.02mol) in agate mortar for 15 minutes which resulted in the formation of complexes. The product (Scheme 1) obtained was then washed with n-hexane to remove unreacted guanine because guanine is soluble in it to obtained pure complexes and resulting complexes were then dried in vacuo using modified procedure reported by (Gianmarco and Catherine, 2020).

Anti-Microbial Activity

The heterocyclic ligand and its metal complexes were screened for antimicrobial activity against four pathogenic bacterial strains (*Streptococcus pyogens, Bascillus subtilus, Selmonella typhi* and *Klebsella pneumoniae*) and two fungal isolates *(Aspergillus fumigatus* and *Candida albicans species)* by the agar well diffusion method. The wells were dug in the media with the help of a sterile metallic borer. The bacteria strains were spread on the surface of the nutrient agar, while the fungal isolates were spread on the potato dextrose agar using the sterile cotton swab. The recommended concentration of the test sample in DMSO was introduced in the respective wells. Other well supplemented with the standard antibacterial drug and antifungal drug respectively, to serve as positive controls. The plates were incubated at 37ºC for 24h in the case of bacteria and 37ºC for 48h in the case of fungi. The activity was determined by measuring the diameter of zones showing complete inhibition in (mm) (Pooja *et al*., 2020).

Determination Anti-Oxidant Property

The method reported by Saif *et al*. (2016) was adopted with little modifications. Serial dilutions were carried out with stock solutions (1mg/ml) of free ligand and its metal complexes and were mixed with DPPH solution in the ratio of 1:4. The mixture was allowed to stand for 30 min in darkness, for the reaction to occur in methanol to obtain concentrations of 1000, 500, 250, 125, 61.5, 31.25, 15.6 and 7.8 µg/mol. The absorbance was recorded at 517nm using a JASCO model V-550 UV-Vis's spectrophotometer. The values were used to calculate the % inhibition, the calculated % inhibition (Equation 1) and various concentrations values of the prepared solutions were statistically analyzed using IBM SPPS software probit analysis to obtained IC_{50}.

$$\%\ \boldsymbol{Inhibition} = \frac{\boldsymbol{Abs\ of\ Control - Abs\ of\ Sample}}{\boldsymbol{Abs\ of\ Control}}\ \boldsymbol{x}\ \mathbf{100} \quad (1)$$

DPPH (2,2-diphenyl-1-picrylhydrazyl) radical scavenging assay is based on reduction of the free radical by an oxidant whereby the DPPH radical with an absorption maximum of 515nm is converted into a colourless compound after reduction.

RESULTS AND DISCUSSION

The complexes produce from the interaction of guanine and metal(II) carbonate were found to be coloured due to charge transfer, the difference in colour may be due light absorption at various wave length. The proposed structure of the complexes is as given in Fig. 1.

$$2C_5H_5N_5O + MCO_3 \longrightarrow [(C_5H_4N_5O)_2M] + H_2O + CO_2$$

M= Mn, Ni, Zn

Scheme 1: general procedure of guanine complexes synthesis

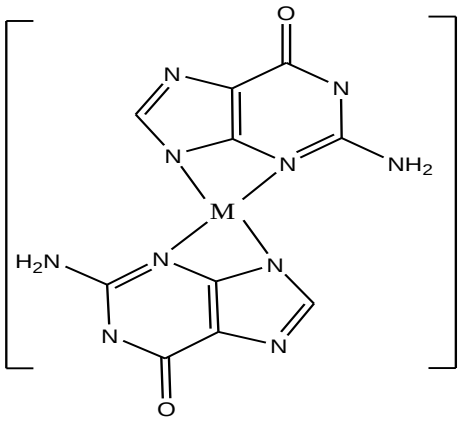

Where M= Mn (II), Ni (II), Zn (II)

Fig 1: Proposed structure of guanine complexes

Table 1. IR Spectral Data of the Metal(II) Complexes

Complexes/ligand	*v*(C=N) cm^{-1}	*v*(M-N) cm^{-1}	*v*(M-N)cm^{-1} ring	*v*(C=O)cm^{-1}	*v*(NH_2) cm^{-1}	*v*(NH) cm^{-1}
Guanine	1674			1696	3312	
$[Mn(C_5H_5N_5O)_2]$	1640	604	450	1700		3137
$[Ni(C_5H_5N_5O)_2]$	1637	582	440	1696		3149
$[Zn(C_5H_5N_5O)_2]$	1640	574	407	1693		3152

The infra-red spectral result (Table 1) of guanine shows a band at 1674cm^{-1} which is associated to v (C=N) stretching. The complexes of guanine with the respective metals shows a stretching at Manganese (1674cm^{-1} to 1640cm^{-1}), so also in nickel (1674cm^{-1} to 1637cm^{-1}) and zinc (1674cm^{-1} to 1640cm^{-1}) are associated with v(C=N) stretching. A slight shift was also observed in v(C=O) in the complexes of Manganese (1674cm^{-1} to 1700cm^{-1}), so also in nickel (1696cm^{-1} to 1696cm^{-1}) and zinc(1696cm^{-1} to 1693cm^{-1}) are associated with v(C=O) stretching. The appearance of new band at Mn (604cm^{-1}) likewise in Ni(582cm^{-1}) and Zn(574cm^{-1}) which were associated with v(M-N) due to deprotonated amino group (NH_2 to NH) respectively. The deprotonated NH stretching appears at Mn (3137cm^{-1}) likewise in Ni (3149cm^{-1}) and Zn (3152cm^{-1}) when compared with those reported by Zaky and Fekri (2019) (3240-3441 cm^{-1}).

Comparing the bands in the ligand to that of the metal complexes shows that there is a shift to lower or higher frequencies which is an indication of complexation between the ligand and the metal ions, Also in the complexes the appearance of new band due to v(M-N) confirms complexation. The wave lengths are compared with those reported by Thamer *et al*. 2022. (405-688) cm^{-1}. The Far-IR spectra of the complexes showed bands in the regions 574−550 cm^{-1} and 486−479 cm^{-1}, which were assigned to ν(M−N) and ν(M−O) stretching vibrations respectively, which were within the range (405-688) cm^{-1} reported by Thamer *et al*. (2022).

Furthermore, the appearance of new bands; at Mn (450cm^{-1}), Ni (440cm^{-1}) and Zn (407cm^{-1}) which were associated with v(M-N) due to azomethane nitrogen (ring nitrogen) respectively, compares closely with those reported by Thamer *et al*. (2022).

Table 2: Decomposition Temperature/Melting Point Temperature of Guanine and Its Metal (II) Complexes

Ligand/complexes	Colour	Decomposition/melting point Temp. (^OC)
Guanine		360
$[Mn(C_5H_5N_5O)_2]$	Creamy white	Greater than 460
$[Ni(C_5H_5N_5O)_2]$	Light green	Greater than 480
$[Zn(C_5H_5N_5O)_2]$	White	Greater than 485

The guanine ligand (Table 2) which is white in colour, having a melting point temperature of 360°C.

The interaction of guanine with respective divalent metal salts (Table 2) yielded coloured complexes, due to electronic transition from lower to higher energy level except zinc. Manganese, nickel and zinc complexes are creamy white, light green and white, the difference in colour is due absorption of light at different wave length, with

decomposition temperature above 360oC, the high decomposition temperature of the complexes as compared to the ligand may be due the coordination between the central metal ion and the ligand (metal-nitrogen bond), size of metal (the smaller the metal the higher the ionization potential), ring size and cornical structure.

Table 3: Molar Conductivity of Guanine Metal(II) Complexes

Ligand/complexes	Specific Conductance (Ohm^{-1} cm^{-1})	Molar conductivity ($\Omega^{-1}cm^2$ mol^{-1})
Guanine		-
$[Mn(C_5H_5N_5O)_2]$	$1.41x10^{-6}$	1.41
$[Ni(C_5H_5N_5O)_2]$	$1.80\ x10^{-6}$	1.80
$[Zn(C_5H_5N_5O)_2]$	$1.50\ x10^{-6}$	1.50

Molar conductance (Table 3) of the complexes were determined using JENWAY 4010 conductivity meter (10^{-3}M) in DMSO solution which lies within the range of $29.0 - 60.6 \times 10^{-6}$ $\Omega^{-1}cm^2$ mol^{-1}, The lower value indicate that they are non-electrolyte according to Zaky and Fekri (2019) and Tadewos *et al*. (2022).

Table 4: Magnetic Susceptibility of guanine Complexes

Ligand/complexes	Xg($gmol^{-1}$)	Xm($gmol^{-1}$)	$\mu_{eff\ (BM)}$	N	Property
Guanine					
$[Mn(C_5H_5N_5O)_2]$	$1.18\ x10^{-4}$	4.19×10^{-2}	6.4	5	Paramagnetic
$[Ni(C_5H_5N_5O)_2]$	$1.89\ x10^{-6}$	6.78×10^{-4}	3.3	2	Paramagnetic
$[Zn(C_5H_5N_5O)_2]$	$-3.75\ x10^{-7}$	-1.4×10^{-4}	-Ve	-	Diamagnetic

$$\mu\mathbf{eff} = \sqrt{n(n+2)} \qquad (2)$$

The results of magnetic moment (Table 4) value of the transition metal complexes were calculated using equation 2 which shows magnetic moment of Mn (II) to be 6.4B.M, Ni (II) to be 3.3B.M and Zn (II) negative complex is consistent with the tetrahedral geometry (sp^3) which correspond to 5, 2 and zero (0) unpaired electron respectively. The Electronic spectra and magnetic susceptibility measurements indicates that they are square planar complexes. Also, suggest their structure in which (NH_2 and N=N) group acts as bidentate ligand when compared with Jitendra *et al*. (2021).

Table 5: Elemental Analysis of Guanine and Its Metal(II) Complexes

Ligand/complexes	Carbon calculated (experimental)	Hydrogen calculated (experimental)	Nitrogen calculated (experimental)
Guanine	39.73(39.63)	3.31(3.29)	46.36(46.30)
$[Mn(C_5H_5N_5O)_2]$	33.80(33.63)	2.25(2.20)	39.44(39.30)
$[Ni(C_5H_5N_5O)_2]$	33.43(33.33)	2.23(2.10)	38.99(38.52)
$[Zn(C_5H_5N_5O)_2]$	32.81(32.72)	2.19(2.12)	38.27(38.16)

The elemental analysis (Table 5) revealed that the percentage of the elements in guanine were found to be; nitrogen 46.36 (46.30) %, carbon 39.73 (39.63) % and hydrogen 3.32 (3.29) % respectively, in which the values are in the form of theoretically (experimentally). However, the calculated percentages were found to be 46.36%, 39.73% and 3.31%, for nitrogen, hydrogen and carbon respectively.

Also, the elemental analysis (Table 5) revealed that the percentage of nitrogen, carbon and hydrogen in guanine complexes was theoretically (experimentally) to be manganese complex nitrogen 39.44 (39.30)% carbon 33.80 (33.63) % and hydrogen 2.25 (2.20) % so also in Nickel complex nitrogen 38.99 (38.52)%, carbon 33.43 (33.33)% and hydrogen 2.19 (2.10)% respectively, meanwhile in zinc complex nitrogen 38.27(38.16)%, carbon 32.81 (38.72)% and hydrogen 2.19 (2.12) % respectively. The elemental analysis results are consistent with the proposed formula of the complex as it is evident from the comparison of the calculated and the actual values that the difference is always less than one, which suggest that the metal-ligand ratio (M: L) is 1:2 of the element studied as compared with those reported by Aneta *et al*. (2021).

The solubility of guanine and its corresponding metal complexes was also determined in different solvents. The ligand is slightly soluble in acetone, water and DMF but soluble n-hexane and DMSO while insoluble ethanol, methanol, diethylether, benzene and chloroform. The complexes were all slightly soluble in water, DMF, DMSO, ethanol, methanol and diethylether.

Table 6A: Anti-Bacterial Activity of guanine and its complexes Inhibition Zones

	S. payogens				*B. subtilis*			
Concentrations (µg/disk)	4000	2000	1000	500	4000	2000	1000	500
Guanine	15	12	12	10	12	12	12	10
$[Mn(C_5H_5N_5O)_2]$	16	15	16	15	12	10	12	10
$[Ni(C_5H_5N_5O)_2]$	14	11	14	11	17	14	17	14
$[Zn(C_5H_5N_5O)_2]$	16	14	16	14	13	14	13	10
Ciprofloxacin	30							28

Table 6B: Anti-Bacterial Activity of guanine and its complexes Inhibition Zones

Concentrations (µg/disk)	*S. typhi*				*K. neumoniae*			
	4000	2000	1000	500	4000	2000	1000	500
Guanine	14	12	14	12	16	14	16	14
$[Mn(C_5H_5N_5O)_2]$	16	13	16	13	15	15	15	11
$[Ni(C_5H_5N_5O)_2]$	13	13	13	9	17	17	17	14
$[Zn(C_5H_5N_5O)_2]$	11	9	11	9	14	14	14	12
ciprofloxacin				25				31

Table 7: Anti-fungal Activity of guanine and its complexes Inhibition Zones

Concentrations (µg/disk)	*C. albicans*				*A. fumigatus*			
	4000	2000	1000	500	4000	2000	1000	500
Guanine	13	10	13	10	15	15	15	11
$[Mn(C_5H_5N_5O)_2]$	13	10	13	10	12	12	12	11
$[Ni(C_5H_5N_5O)_2]$	14	14	14	11	11	11	11	10
$[Zn(C_5H_5N_5O)_2]$	12	11	12	11	16	16	16	13
Ketoconazole				29				26

KEY: *S. pyogenes: Streptococcus pyogenes* *B. subtilis: Bacillus subtilis*
S. typhi: Salmonella typhi *K. pneumoniae: Klebsiella pneumoniae*
C. albicans: Candida albicans *A. fumigatus: Aspergillus fumigatus*

Antimicrobial agents interfere with cell wall and protein syntheses, metabolic pathways, membrane function, ATP and nucleic acid syntheses. Gram-positive bacteria have a porous peptidoglycan layer and a single lipid bilayer, while Gram-negative bacteria have a double lipid bilayer. Guanine and its metal complexes were found to be active against all tested bacteria and fungi (Table 6A, 6B and 7). Chelation increases the activity of these complexes, leading to decreased coordination polarity and increased lipophilicity. These compounds inhibit bacterial and fungal growth by binding to enzymes involved in biochemical activities, such as protein synthesis and cell respiration. The higher activity of the Ni complex of guanine suggests that coordination increases the lipophilicity of the complex when compared with Muhammad *et al.* (2018) of 1.0-128 µgmL^{-1}.

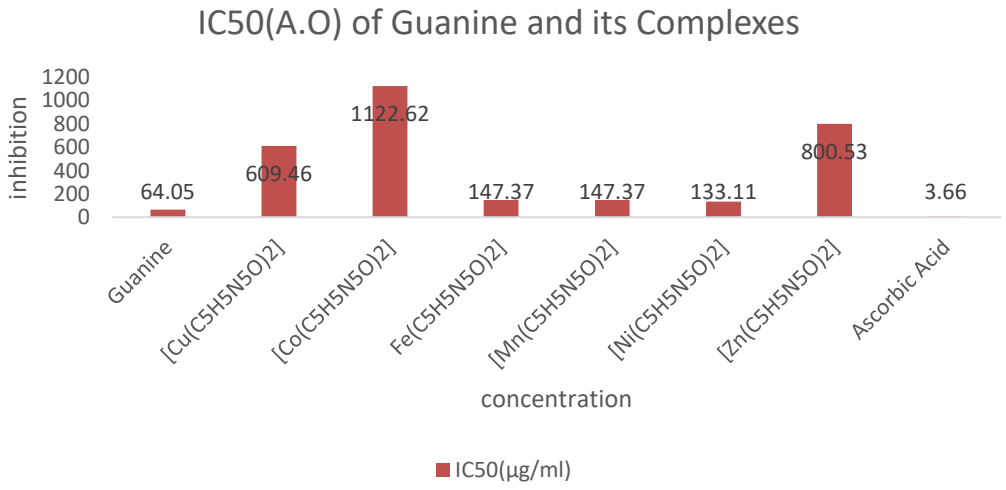

Fig. 2: Graphical representation of anti-oxidant activity of guanine and its complexes

The half-maximal inhibitory concentration (IC50) is a crucial measure of a drug's efficacy, indicating the amount needed to inhibit a biological process by half. It's used in pharmacological research to measure the potency of an antagonist drug. The IC50 value of an antioxidant compound is inversely proportional to its antioxidant activity.

The guanine and its complexes were evaluated for their ability to quench the DPPH (Fig. 2), which is one of the few stable organic nitrogen radicals and bears a purple colour. This assay is based on the measurement of the loss of DPPH after reaction with samples. It is considered as the prior mechanism involved in the electron transfer. The IC50 value is calculated as the concentration of antioxidants needed to decrease the initial DPPH concentration by 50%. Thus, the lower IC50 value the higher antioxidant activity. The guanine showed an antioxidant activity (IC50 = 64.05µg/ml) comparable to the reference ascorbic acid (IC50 = 3.66µg/ml) shows that it is moderately active. On complexing with the corresponding metals shows Mn(II) (IC50 = 64.05µg/ml), also Ni(II) (IC50 = 133.11µg/ml) and Zn(II) (IC50 = 800.53µg/ml). The lowest antioxidant activity corresponds Zn(II) complex is inactive while the highest correspond to Mn(II) (IC50 = 64.05µg/ml) complex which fall within the range (0.00 – 100µg/ml) reported by Fausto *et al.* (2020), Brondwyn and Janice, (2022).

CONCLUSION

Complexes of metal(II) (Mn, Ni, Zn) with heterocyclic based ligand guanine were successfully synthesized via Mechanochemical method. The chemical structures of complexes were studied by the use of physical methods such as solubility, decomposition/melting point temperature (180°C to above 360°C) indicated the stability of the new complexes, conductivity measurement with low values indicates that the synthesized complexes are non-electrolytes, magnetic susceptibility indicating paramagnetic (unpaired electron) and diamagnetic(paired electrons) with tetrahedral geometry, they complexes are found to be coloured due light absorbance at various wavelength elemental analysis show that the complexes are successfully synthesized.

In general, all these complexes showed highest inhibition zones at highest concentration in all the bacteria and the fungi due to increase in polarity which increase lipophilicity. The antioxidant study reveals that the complexes are active due low IC50 value. In general, affording solid state synthesis of inorganic complexes will lead to a greener environment and time consuming using old method will be avoided.

REFERENCES

Abdulaziz M. A, Ahmed .K. H., Ziyad. A. T., Waleed. A. (2019). Synthesis, Characterization and Biological and Catalytic Activities of Propionitril: Ligated Transition Metal Complexes with [B(C6F5)4] as Counter Anion. *Catalysis Letters* 149(17):2317 – 2324.

Brondwyn S. McGhie and Janice R. Aldrich-Wright (2022). Photoactive and Luminescent Transition Metal Complexes as Anticancer Agents: A Guiding Light in the Search for New and Improved Cancer Treatments. *Biomedicines*, 10, 578. https://doi.org/10.3390/biomedicines10030578.

Fausto, R. J., Jessica, G. P., José, P. C. Jazmin, M. P. R., Ajit, K. P. Gloria. D. R. and Blanca, E. R. (2020). Phytochemical Constituents, Antioxidant, Cytotoxic, and Antimicrobial Activities of the Ethanolic Extract of Mexican Brown Propolis. *Antioxidants*, 9, 70.

Haoqin. Z. and Zhiyou. W. (2019). Solid-State Anaerobic Digestion for Waste Management and Biogas Production. *Adv Biochem Eng Biotechnol*. DOI: 10.1007/10_2019_86.

Irina. G. M. and Constantin. A. (2021). Analytical Methods Used in Determining Antioxidant Activity: A Review. *Int. J. Mol. Sci*., 22, 3380.

Muhammad A., Farooq, A., Mahmood, A., Abdul Karim. K., Alkharfy. M., Anwarul. H. G. (2018). Free Mechano-chemical Synthesis of New Omeprazole Derived Metal Complexes: Characterization, Urease Inhibitory Kinetics and Selective Anti-Helicobacter pylori Activity. *Bentham Science* 15(3): 240 – 250.

Najma, A. Fithri, F., Tia, S., Atika, A., Diva, Y. (2019). Antioxidant Activity Analysis and Standardization of Parkia speciosa (Petai) Pods Ethanol Extract. *J. Science and Technology Indonesia* 4(1):5 - 10. https://doi.org/10.26554/sti

Nattaya. T., Pinya .M., Ruangdaj. T. (2017). *Fe-Sn* Intermetallic Compound Synthesized via Mechanical Alloying and Liquid Phase Sintering. *J. Natural Sciences* 16(4):239-253.

Panel, S. M., Pinar, S., Olawale, L. O,. Tebello. N. (2021). *The antibacterial and antifungal properties of neutral, octacationic and hexadecacationic Zn phthalocyanines when conjugated to silver nanoparticles Photodiagnosis and Photodynamic Therapy. ELSEVIER*, Volume 35, 102361

Pooja, S., Rajshree, K., Renuka, C., (2020). Complexes of Pyrimidine Thiones: Mechanochemical Synthesis and Biological Evaluation. *Asian Journal of Chemistry;32(10), 2594-2600.*

Rina T. (2022). Mechanochemical Synthesis of Organometallic Compounds and Their Applications to Organic Synthesis Hokkaido University Graduate School of Chemical Sciences and Engineering Organoelement Laboratory. Ph.D thesis.

Resat, A., Mustafa, O., Kubilay, G. and Esra, C. (2016). Antioxidant Activity/Capacity Measurement. 1. Classification, Physicochemical Principles, Mechanisms, and Electron Transfer (ET)-Based Assays food. *Journal of Agriculture and Food Chemistry*, pubs.acs.org/JAFC, 64, 997−1027.

Siffeen, Z., Thierry, R. and Farukh A. (2019). *Enantiomeric Amino Acid Schiff Base Copper(II) Complexes as a New Class of RNA-Targeted Metallo-Intercalators: Single X-ray Crystal Structural Details, Comparative in Vitro DNA/RNA Binding Profile, Cleavage, and Cytotoxicity*. ACS Omega, 4, 7691−7705.

Sudip. M., Thanawat. C., Rapheepraew. S., Rungthip .K., Sasikarn. H., Preeyanuch. S. and Vuthichai. E. (2016). *Solid–state Synthesis of Polyhedral Oligomeric Silsesquioxane-Supported N-Heterocyclic Carbenes/Imidazolium salts on Palladium Nanoparticles: Highly Active and Recyclable Catalyst.* Materials Science inc. Nanomaterials & Polymers. *ChemistrySelect* 2016, 1, 5353 – 5357.

Tadewos, D., Digafie, Z., Tegene, D., Taye B. D., Rajalakshmanan, E. (2022). *Synthesis, Characterization, and Biological Activities of Novel Vanadium (IV) and Cobalt (II) Complexes*. ACS Omega 2022, 7, 4389−4404

Thamer A. A., Ahmed N. A, El-Sayed S. S., Ebtesam. H. L. A., Abuzar E. A. (2022). Synthesis, characterization, and anticancer activity of some metal complexes with a new Schiff base ligand. *Arabian Journal of Chemistry* 15, 103559.

Zaky R, Fekri A. (2019). *Ball milling: a green mechanochemical approach for synthesis of Ni (II), Co (II) and Cu (II) complexes*. *Appl Organometal Chem*.; e4786. https://doi.org/10.1002/aoc.4786

Zuofa. Z., Guoying. L., Huijuan. P., Leifa. F., Carlos. R. S., Ashok. P. (2012). *Production of Powerful Antioxidant Supplements via Solid-State Fermentation of Wheat (Triticum aestivum Linn.) Food Technol. Biotechnol.* 50 (1) 32–39.